Proceedings of the 1998 Conference on Information Sciences and Systems

---

Volume II

Department of Electrical Engineering
Princeton University
Princeton, New Jersey 08544-5263

Intensity/Cross-Phase/Intensity Conversion Filters in Dispersion Compensated Multiwavelength Transmission Systems.

Giovanni Bellotti, Matteo Varani, Cristian Francia and Alberto Bononi
Università di Parma – Dipartimento di Ingegneria dell'Informazione – Viale delle Scienze, I-43100 Parma, Italy
phone: +39-521-905-760 fax: +39-521-905-758 – email: bellotti@tlc.unipr.it, bononi@tlc.unipr.it

Abstract— In this paper we present an entirely linear model to accurately predict the phase and intensity distortion induced by the nonlinear effect of cross-phase modulation in dispersion compensated optical systems.

As shown in [1], cross-phase modulation on each channel of a wavelength-division multiplexed transmission system can be viewed as a phase modulation, where the modulating signal is the sum of the input intensities of all the other co-propagating channels, each filtered by a low-pass filter, dependent on the walk-off parameter.

We give an explicit expression of the impulse response of such filter in the general case of dispersion compensated systems and we show by simulation that, in the case of intensity-modulated transmission, it gives an optimal prediction of the signal phase, even when the underlying assumption of negligible envelope distortion, upon which its derivation is based, is violated.

Finally, we introduce a new model of the joint effect of cross-phase modulation and group-velocity dispersion in compensated systems, leading to a linear filter that, applied to the input intensities of the co-propagating channels, gives a very good approximation of the signal envelope at the end of the system.

I. Introduction

In a fundamental paper, Chiang et al. [1] have shown that cross-phase modulation (XPM) in wavelength-division multiplexed (WDM) optical transmission systems can be modeled as a phase modulator with inputs from the intensity of co-propagating waves. Such inputs are lowpass filtered by the relative channel walk-off induced by chromatic dispersion, the larger the walk-off, the narrower the filter bandwidth. The model nicely explains the weak dependence of XPM on the number of WDM channels, already observed experimentally and by simulation in [2]. Chiang et al. [1] have extended such model to cascades of ideally amplified fiber links with dispersion compensation.

This paper provides a time-domain derivation of the theoretical model proposed in [1], leading to an explicit expression for the impulse response of such intensity-modulation/cross-phase modulation (IM/XPM) filter, both for a single fiber span and for a cascade of amplified links with dispersion compensation. Incidentally, we find that the expression of the filter phase in [1] is incorrect because of an inconsistency in the use of Fourier transforms.

Having the correct phase expression, we show that such filter is non-causal when the interfering channel travels faster than the observed channel. In such case, the phase of the interfering channel at the detector contains information about the future information bits of the observed channel.

We give a graphical interpretation of the filter impulse response in the case of link-by-link dispersion compensation in a cascade of amplified links, so that the periodic forward and backward relative walk-off becomes apparent.

For the case of intensity-modulation direct-detection (IM/DD) systems, we provide simulation evidence that the model surprisingly holds even though the assumption of negligible envelope distortion upon which its derivation is based is strongly violated. In other words, we find that the modulation induced on the optical field phase by XPM is nearly independent of the distortion induced on the intensity of the optical field by group velocity dispersion (GVD). This is due to the above-mentioned lowpass filtering effect of channel walk-off on XPM.

Like any phase noise, XPM generates envelope distortion at the end of the transmission fiber because of the phase-to-intensity (PM/IM) conversion caused by GVD [3]. However, its distributed generation makes XPM different from classical phase noise. While the PM/IM distortion induced by a phase noise present at the *input* of a transmission fiber can be perfectly undone by a compensating fiber of suitable length, the PM/IM distortion induced by the XPM components generated away from the input cannot be perfectly compensated. To capture the distributed nature of the XPM effect, we think of the transmission fiber as a sequence of infinitesimal segments. By the IM/XPM model we can accurately predict the XPM component generated in each segment, and thus we can predict the GVD-induced PM/IM contribution of that XPM component to the total intensity distortion at the end of the compensated link. Assuming the contributions of each segment add up, we obtain in the limit a linear filter capturing the distributed IM/XPM/IM conversion, and giving a very good prediction of the XPM induced envelope distortion.

The paper is organized as follows. Section II. provides the derivation of the IM/XPM filter impulse response both for the case of a single link, and for the general one of dispersion-compensated cascades of amplified fiber links. Section III. proposes the original theoretical model capturing the essence of the interaction between XPM and GVD, and shows the derivation of the IM/XPM/IM filter. Section IV. presents simulation results providing evidence that the model represented by the IM/XPM filter holds even in the presence of strong intensity distortion due to GVD, and that the IM/XPM/IM filter gives a very good approximation of the XPM induced intensity distortion. Finally, section V concludes the paper.

II. IM/XPM Conversion Filter

A. Single Span

We consider a WDM system composed of one span of single-mode optical fiber, with N co-propagating channels having the same polarization.

The nonlinear Schrödinger equation describing the propagation along the z axis of the complex envelope $A_s(z,t)$ of the reference channel s ($s = 1, \cdots, N$) is [4]:

$$\frac{\partial A_s(z,t)}{\partial z} + \frac{1}{v_{gs}}\frac{\partial A_s(z,t)}{\partial t} + \frac{\alpha}{2}A_s(z,t) = \\ = -j\gamma A_s(z,t)\left[|A_s(z,t)|^2 + 2\sum_{p\neq s}|A_p(z,t)|^2\right] \quad (1)$$

where v_{gs} is the group velocity of channel s, α is the attenuation coefficient, γ is the nonlinearity coefficient and the summation is extended to the set of channels $\{p = 1, \cdots, N \ : \ p \neq s\}$. The two terms on the right hand side of (1) give rise to self-phase modulation (SPM) and XPM, respectively. The $-j$ term in (1) appears because of the engineering definition of Fourier transforms [4]. A $+j$ term appears when using the physicist notation [5].

Note that the contributions giving rise to four wave mixing (FWM) have been omitted from the right hand side of the equation. Thus we suppose to be working with high local GVD, as common in dispersion mapping [6],[7] to effectively suppress FWM.

Note also that on the left hand side of (1) we have neglected the higher order time derivatives of $A_s(z,t)$, which cause the GVD-induced distortion of the envelope. It is only under this assumption that equation (1) can be solved exactly, giving the field at the fiber output as:

$$A_s(L,t) = A_s(0, t - L/v_{gs})e^{-\frac{\alpha L}{2}}e^{j\theta_s(L,t)} \quad , \quad s = 1, \cdots, N \quad (2)$$

where L is the fiber length and the signal phase is [1]:

$$\theta_s(L,t) = \theta_0 - \gamma\left[L_{eff}(L)\left|A_s\left(0, t - \frac{L}{v_{gs}}\right)\right|^2 + \right. \\ \left. + 2\sum_{p\neq s}\int_0^L \left|A_p\left(0, t - \frac{L}{v_{gs}} + d_{sp}z\right)\right|^2 e^{-\alpha z}dz\right] \quad (3)$$

where θ_0 is the initial phase, and $L_{eff}(L) = \frac{1-e^{-\alpha L}}{\alpha}$ is the effective length of the fiber. The two terms in the squared bracket represent SPM and XPM, respectively.

The coefficient $d_{sp} = v_{gs}^{-1} - v_{gp}^{-1} \simeq D\Delta\lambda_{sp}$ [5] is the *walk-off* parameter between channels s and p, where D is the dispersion coefficient of the fiber and $\Delta\lambda_{sp}$ is the wavelength distance between the two channels.

This is the case studied in [1] in the frequency domain, using sinusoidally modulated signals. Here we proceed instead in the time domain. With the variable change $\tau = -zd_{sp}$, the term related to XPM in (3) can be rewritten as:

$$\theta_s^{\text{XPM}}(L,t) = \\ -2\gamma\sum_{p\neq s}\frac{1}{d_{sp}}\int_{-d_{sp}L}^0 \left|A_p\left(0, t - \tau - \frac{L}{v_{gs}}\right)\right|^2 \exp\left[\alpha\frac{\tau}{d_{sp}}\right]d\tau \quad (4)$$

The above variable change has a physical meaning: integrating in (3) in the space domain, is equivalent to integrate, in the time domain, that part of the $A_p(0,t)$ interfering signal which crosses the reference signal $A_s(0,t)$ during the propagation over distance L. The relative walk-off between the s and the p channel is d_{sp} [s/m], so that the integral in the time domain has to be extended over a duration $|d_{sp}|L$, as in (4). In (4) we recognize the following convolution integral:

$$\theta_s^{\text{XPM}}(L,t) = -2\gamma\sum_{p\neq s}P_p\left(0, t - \frac{L}{v_{gs}}\right) \otimes h_{sp}(t) \quad (5)$$

where $P_p(0,t) = |A_p(0,t)|^2$ is the input power of signal p and $h_{sp}(t)$ is the impulse response of a linear filter $h_{sp}(t)$, which, for both $d_{sp} > 0$ and $d_{sp} < 0$, is given by:

$$h_{sp}(t) = \frac{1}{|d_{sp}|}e^{\alpha\frac{t}{d_{sp}}}\ \Pi\left(\frac{t + d_{sp}L/2}{L|d_{sp}|}\right) \quad (6)$$

where we have used the rectangular function $\Pi\left(\frac{t}{\tau}\right) \triangleq 1$ for $|t| < \tau/2$, and zero outside.

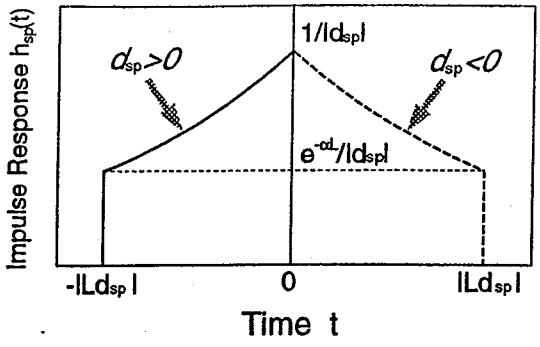

Fig. 1. Impulse response $h_{sp}(t)$ in both cases of positive and negative walk-off parameter.

In Fig. 1 we plot the impulse response $h_{sp}(t)$, for both $d_{sp} > 0$ and $d_{sp} < 0$. Note that when $d_{sp} > 0$, $h_{sp}(t)$ is non-causal. This should not surprise, since the p signal travels faster than s, so that during propagation $\theta_s(z,t)$ is affected by the future bits of the p signal.

The peak of $h_{sp}(t)$ near the origin is due to the fact that the p channel is attenuated during propagation, so that the XPM effect is stronger at the beginning of the interaction. When the fiber has no attenuation ($\alpha = 0$), $h_{sp}(t)$ reduces to a rectangle. In the case of no channel walk-off ($d_{sp} = 0$), we have $h_{sp}(t) = L_{eff}(L)\ \delta(t)$, so that we get the well-known formula $\theta_s^{\text{XPM}}(L,t) = -2\gamma L_{eff}(L)\sum_{p\neq s}P_p\left(0, t - \frac{L}{v_{gs}}\right)$.

The Fourier transform of the impulse response (6) is:

$$H_{sp}(\omega) = \int_{-\infty}^{\infty} h_{sp}(t)e^{-j\omega t}dt = \frac{1 - e^{-(\alpha - j\omega d_{sp})L}}{\alpha - j\omega d_{sp}} \quad (7)$$

Its squared magnitude and phase are, respectively:

$$|H_{sp}(\omega)|^2 = \frac{L_{eff}^2(L)}{1 + (\omega d_{sp}/\alpha)^2}\left[1 + \frac{4e^{-\alpha L}\sin^2(\omega d_{sp}L/2)}{(1 - e^{-\alpha L})}\right] \quad (8)$$

$$\angle H_{sp}(\omega) = \text{arctg}\left(\frac{\sin(\omega d_{sp}L)}{\cos(\omega d_{sp}L) - e^{\alpha L}}\right) + \text{arctg}\left(\frac{\omega d_{sp}}{\alpha}\right) \quad (9)$$

Equation (8) agrees with the result in [1]. However (9) gives the correct expression for the phase, while expression (10) of [1] is incorrect [1].

From (8) we immediately get the 3-dB bandwidth B_w for fiber length $L \gg 1/\alpha$. In such case the square bracket reduces to 1, and by inspection we see that $B_w = \alpha/|d_{sp}|$. In the limit $d_{sp} \to \infty$ only the DC component is passed by the filter, so that no XPM is observed.

Since B_w quickly decreases with $\Delta\lambda_{sp}$, more distant channels are more filtered and give a lower contribution to XPM. This justifies the experimental observation [2] that XPM does not increase linearly with the number of channels N.

B. Cascade of Amplified Links

In this subsection we analyze XPM in the general case of a system composed of $M-1$ amplifiers, and M links, as in Fig. 3(a). We suppose that the m-th amplifier has gain $G_p^{(m)}$ at the p-th wavelength, so that the channel power, after the m-th amplifier, is $P_p(L_m,t) = [P_p(L_{m-1},t)e^{-(\alpha_m l_m)}]G_p^{(m)}$, where α_i and l_i are the attenuation coefficient and the length of the i-th link, respectively, and $L_m \triangleq \sum_{i=1}^{m} l_i$. The total fiber length is $L = L_M$.

Since, as seen in (3), XPM is given as an integral over the link span, by the linearity of the integral the total XPM at the end of the link can be written as

$$\theta_s^{\text{XPM}}(L,t) = \sum_{i=1}^{M} \theta_s^{\text{XPM}}(l_i,t) \qquad (10)$$

where $\theta_s^{\text{XPM}}(l_i,t)$ is the XPM contribution over the i-th link.

Now it is convenient to write (5) in a time reference moving with velocity v_{gs}:

$$\theta_s^{\text{XPM}}(l_i,t) = -2\gamma \sum_{p\neq s} P_p(0,t) \otimes h_{sp}^{(i)}(t) \qquad (11)$$

where the superscript (i) indicates the dependence of the impulse response $h_{sp}(t)$, defined in (6), on the length, walk-off and attenuation parameters $l_i, d_{sp}^{(i)}, \alpha_i$ of the i-th link.

The XPM at the end of the first link is $\theta_s^{\text{XPM}}(l_1,t) = -2\gamma \sum_{p\neq s} P_p(0,t) \otimes h_{sp}^{(1)}(t)$. The XPM contribution of the second link is:

$$\begin{aligned}\theta_s^{\text{XPM}}(l_2,t) &= -2\gamma \textstyle\sum_{p\neq s} P_p(l_1,t) \otimes h_{sp}^{(2)}(t) \\ &= -2\gamma \textstyle\sum_{p\neq s} e^{-\alpha_1 l_1} G_p^{(1)} P_p(0, t+l_1 d_{sp}^{(1)}) \otimes h_{sp}^{(2)}(t) \\ &= -2\gamma \textstyle\sum_{p\neq s} P_p(0,t) \otimes \left[C_p^{(2)} h_{sp}^{(2)}(t+l_1 d_{sp}^{(1)})\right]\end{aligned} \qquad (12)$$

where $C_p^{(2)} \triangleq e^{-\alpha_1 l_1} G_p^{(1)}$ is the power gain at the beginning of the second link.

From (12) we see that the XPM contribution of the second link can be seen again as a linear filtering of the same input function $P_p(0,t)$. The linear filter is as in (6), but translated in time by $l_1 d_{sp}^{(1)}$ and multiplied by the constant $C_p^{(2)}$. In general, the XPM contribution of the m-th link $(m = 1, \cdots, M)$ is:

$$\begin{aligned}\theta_s^{\text{XPM}}(l_m,t) &= -2\gamma \textstyle\sum_{p\neq s} P_p(L_{m-1},t) \otimes h_{sp}^{(m)}(t) \\ &= -2\gamma \textstyle\sum_{p\neq s} P_p(0,t) \otimes \left[C_p^{(m)} h_{sp}^{(m)}\left(t + \sum_{i=1}^{m-1} l_i d_{sp}^{(i)}\right)\right]\end{aligned} \qquad (13)$$

where the effective gain at the beginning of the m-th link is $C_p^{(m)} \triangleq \prod_{i=1}^{m-1} e^{-\alpha_i l_i} G_p^{(i)}$, and $C_p^{(1)} \triangleq 1$.

By (10), the total XPM at the end of the M-th link is then

$$\begin{cases} \theta_s^{\text{XPM}}(L,t) &= -2\gamma \sum_{p\neq s} P_p(0,t) \otimes \hat{h}_{sp}(t) \\ \hat{h}_{sp}(t) &= \left\{\sum_{k=1}^{M} C_p^{(k)} h_{sp}^{(k)}\left(t + \sum_{i=1}^{k-1} l_i d_{sp}^{(i)}\right)\right\}. \end{cases} \qquad (14)$$

where $\hat{h}_{sp}(t)$ is the overall filter impulse response.

In Fig. 2 we show a block diagram implementing $\hat{h}_{sp}(t)$. The equivalent filter for channel p is indeed a parallel bank of filters.

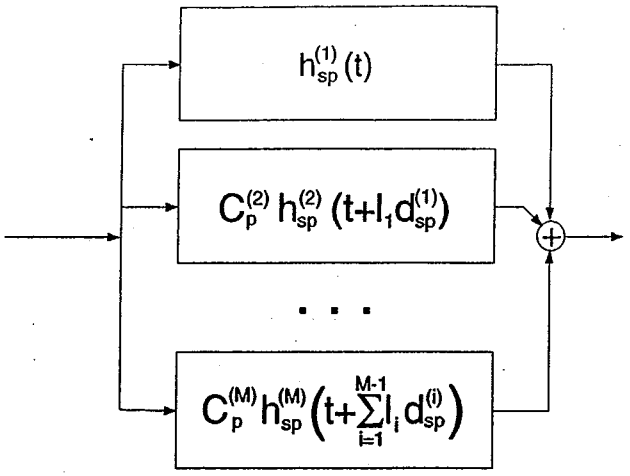

Fig. 2. Block diagram of $\hat{h}_{sp}(t)$ as in (14).

Equation (14) is extremely general. It can be used for any type of multistage system, with any amplifier gain profile, with any kind of compensating scheme.

In Fig. 3(a) we show an example of $\hat{h}_{sp}(t)$ in the case of a non-compensated system, composed of M identical links, when the amplifiers exactly compensate the fiber loss. The overall impulse response is just the sum of the M shifted copies of the basic filter (6).

In Fig. 3(b) we show the case of an imperfectly compensated system, composed of $M = 4$ identical spans of transmission fiber, each followed by a span of compensating fiber of opposite dispersion and an amplifier to exactly recover the span loss. The figure shows the individual contributions of each fiber segment to the overall impulse response. As opposed to (a), note that in (b) the (identical) contributions of the transmission fibers are partially overlapping, because of the backward relative walk-off achieved by the compensating fibers, which bring the s and p channels back aligned, although not exactly. In this example the responses

[1] First, it is has a typo and should read: $\phi = -\arg(-\alpha + i\omega d_{12}) + \arg(-(1 - e^{-\alpha L}\cos(\omega d_{12} L)) + ie^{-\alpha L}\sin(\omega d_{12} L))$, which agrees with (9) here.
Second, there is an inconsistency in [1]: the authors start with a version of equation (1) derived according to the physicists' notation for Fourier transforms [5], and later on they use ([1], eq. (16)) the engineering notation, as we do here. This is the reason why our expression for ϕ in (9) matches with their ϕ. However, in the physicists' notation, the correct expression is $-\phi$.

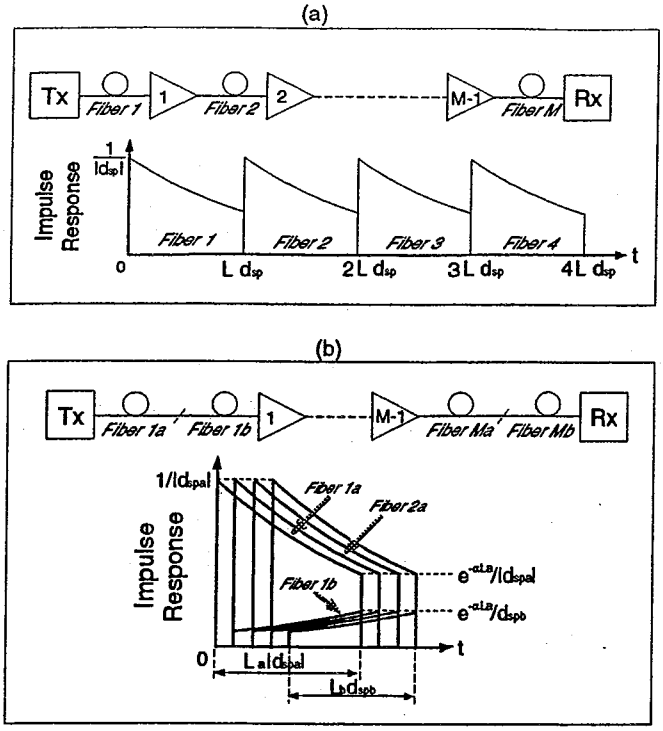

Fig. 3. M amplified fiber links. (a) Uncompensated case; (b) Imperfectly compensated case. Top: scheme; bottom: impulse response of individual fiber sections.

of the compensating fibers are non-causal. The compensating fibers, when placed at the end of each transmission span, give typically only a small contribution to the overall filter response $\hat{h}_{sp}(t)$, and can thus be safely neglected. In the case of a perfectly compensated M-span system, neglecting the contribution of the compensating fibers at each link, we obtain: $\hat{h}_{sp}(t) \simeq M h_{sp}^{(1)}(t)$, so that the XPM effect is M times larger than that of a single link.

III. IM/XPM/IM Conversion Filters

A. Single Uncompensated Span

In this section we will derive a linear filter that predicts the intensity distortion induced by XPM at the end of a single compensated fiber span.

XPM generates envelope distortion at the end of the transmission fiber because of the phase-to-intensity (PM/IM) conversion caused by GVD [3]. While the PM/IM distortion induced by the XPM generated at the *input* of the transmission fiber can be perfectly undone by a compensating fiber of suitable length, the PM/IM distortion induced by the XPM components generated away from the input cannot be perfectly compensated.

To capture the distributed nature of the XPM effect, we think of the transmission fiber as a sequence of Q infinitesimal segments of length Δz, such that $L = Q\Delta z$, as in Fig 2.

In section IV we will show by simulation that the IM/XPM filter (6) gives a very accurate prediction of the phase even when the assumption of undistorted field envelope upon which its derivation is based is strongly violated. Therefore using the IM/XPM filter we can accurately

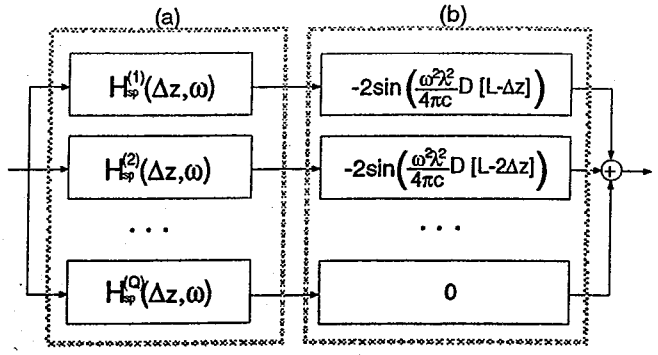

Fig. 4. Excluding block (b): block diagram of eq. 15; with block (b): complete IM/XPM/IM filter.

predict the XPM component generated in each infinitesimal segment. The IM/XPM filter of the n-th segment, $1 \le n \le Q$, is

$$H_{sp}^{(n)}(\Delta z, \omega) = e^{-\alpha(n-1)\Delta z} e^{j\omega(n-1)\Delta z d_{sp}} \frac{1 - e^{-(\alpha - j\omega d_{sp})\Delta z}}{\alpha - j\omega d_{sp}}.$$

Thus we can write the IM/XPM filter of the whole fiber (7) as:

$$H_{sp}(\omega) = \left\{ \sum_{n=1}^{Q} H_{sp}^{(n)}(\Delta z, \omega) \right\} \tag{15}$$

whose block diagram is shown in Fig. 4 (excluding block (b) described next). The Fourier transform of the XPM component generated on the signal s by the p-th interferer in the n-th segment, is thus: $\theta_{sp}^{(n)}(\omega) = -2\gamma H_{sp}^{(n)}(\Delta z, \omega) P_p(0, \omega)$.

Such XPM component now propagates over a distance $L - n\Delta z$ till the end of the fiber, giving a GVD-induced PM/IM power contribution ([3], eq. (29)):

$$\Delta P_{sp}^{(n)}(\omega) = -2 < P_s > \sin\left[\omega^2 \frac{\lambda^2}{4\pi c} D(L - n\Delta z)\right] \theta_{sp}^{(n)}(\omega) \tag{16}$$

where $< P_s >$ is the time averaged signal power, D the dispersion coefficient at the signal wavelength, λ the central wavelength and c the light velocity.

Assuming the contributions of each segment add up to build the total power distortion, we get the total IM/XPM/IM filter shown in Fig. 4 (now including block (b)). In such diagram we can now take the limit for $\Delta z \to 0$ and $Q \to \infty$ (with constraint $L = Q\Delta z$) to get the IM/XPM/IM filter:

$$\begin{aligned} H_{sp}^{\mathrm{IM}}(\omega) &= \lim_{\substack{Q\to\infty, \Delta z\to 0 \\ Q\Delta z = L}} -2 \sum_{n=1}^{Q} \sin\left[\frac{\omega^2\lambda^2}{4\pi c} D(L - n\Delta z)\right] H_{sp}^{(n)}(\Delta z, \omega \\ &= j \left\{ e^{j\frac{\lambda^2}{4\pi c} DL\omega^2} \left(\frac{1 - e^{(-\alpha + j(d_{sp}\omega - \frac{\lambda^2}{4\pi c} D\omega^2))L}}{\alpha - j(d_{sp}\omega - \frac{\lambda^2}{4\pi c} D\omega^2)} \right) \right. \\ &\quad \left. - e^{-j\frac{\lambda^2}{4\pi c} DL\omega^2} \left(\frac{1 - e^{(-\alpha + j(d_{sp}\omega + \frac{\lambda^2}{4\pi c} D\omega^2))L}}{\alpha - j(d_{sp}\omega + \frac{\lambda^2}{4\pi c} D\omega^2)} \right) \right\}. \end{aligned} \tag{17}$$

Finally, the relative XPM-induced signal power variation at the output of the fiber is given by:

$$\frac{\Delta P_s(\omega)}{< P_s >} = -2\gamma \sum_{p \neq s} P_p(0, \omega) H_{sp}^{\mathrm{IM}}(\omega) . \tag{18}$$

Equation (17) has been derived neglecting the higher-order dispersive effects. It is possible to account second-order effects by repeating the previous derivation starting from the model in [8], which is an extension of [3]. Even in this case a closed form of the IM/XPM/IM filter, although more complex, can be obtained [9].

B. Cascade of Amplified Compensated Links

In the case of a cascade of M compensated links, the IM/XPM/IM model can be similarly derived. The only difference is that now the XPM contribution $\theta_{sp}^{(nk)}(\omega)$ generated in the n-th infinitesimal segment of the k-th fiber is converted in intensity variation by the dispersion seen from section n to the end of the overall link. Such residual dispersion is $D_R^{(nk)} = (l_k - n\Delta z)D_k + \hat{D}_R^{(k)}$, where $\hat{D}_R^{(k)} \triangleq \sum_{i=k+1}^{M} D_i L_i$, and D_i is the dispersion coefficient of the i-th fiber at the signal wavelength.

The power variation induced by $\theta_{sp}^{(nk)}(\omega)$ becomes:

$$\frac{\Delta P_{sp}^{(nk)}(\omega)}{<P_s>} = -2\sin\left[\omega^2 \frac{\lambda^2}{4\pi c} D_R^{(nk)}\right] \theta_{sp}^{(nk)}(\omega) \,. \qquad (19)$$

As before, taking limits, the IM/XPM/IM filter relative to the XPM generated in the generic k-th fiber is:

$$H_{sp}^{\mathrm{IM}(k)}(\omega) = \\ = j\left\{ e^{j\frac{\lambda^2}{4\pi c}\left(l_k D_k + \hat{D}_R^{(k)}\right)\omega^2} \left(\frac{1-e^{(-\alpha_k + j(d_{sp}^{(k)}\omega - \frac{\lambda^2}{4\pi c} D_k \omega^2))l_k}}{\alpha_k - j(d_{sp}^{(k)}\omega - \frac{\lambda^2}{4\pi c} D_k \omega^2)} \right) \right. \\ \left. - e^{-j\frac{\lambda^2}{4\pi c}\left(l_k D_k + \hat{D}_R^{(k)}\right)\omega^2} \left(\frac{1-e^{(-\alpha_k + j(d_{sp}^{(k)}\omega + \frac{\lambda^2}{4\pi c} D_k \omega^2))l_k}}{\alpha_k - j(d_{sp}^{(k)}\omega + \frac{\lambda^2}{4\pi c} D_k \omega^2)} \right) \right\} \qquad (20)$$

and the IM/XPM/IM filter over the M links becomes (see (14)):

$$H_{sp}^{\mathrm{IM}}(\omega) = \sum_{k=1}^{M} C_p^{(k)} e^{(j\omega \sum_{i=1}^{k-1} d_{sp}^{(i)} l_i)} H_{sp}^{\mathrm{IM}(k)}(\omega) \,. \qquad (21)$$

The relative signal power variation at the receiver is given again by eq. (18).

IV. Simulations

In Fig. 5 and Fig. 6 we compare the results of computer simulations, performed by the Split-Step Fourier Method [5], with the predictions of our model.

Simulations are carried out for a multi-span WDM system, with 10 spans, 2 channels, 5 dBm peak power per channel, of the compensated type depicted in Fig. 3(b). One of the channels (pump) is on-off keying (OOK) modulated with nonreturn-to-zero (NRZ) pulses at a bit rate $R = 10\ Gb/s$, while the other (probe) is unmodulated. To avoid Gibbs oscillations, the NRZ pulses were simulated as raised cosine pulses with 80% roll-off [10].

Fig. 5 refers to a system in which at each span the transmission fiber is a non-zero dispersion fiber (NZDF), with dispersion $D = -2$ ps/nm/km and length $l = 85$ km, and a standard single-mode fiber (SMF) with $D = 17$ ps/nm/km and length $l = 10$ km is used for span compensation.

Fig. 6 refers to a system in which the transmission fiber is SMF, with dispersion $D = 17$ ps/nm/km and length $l =$

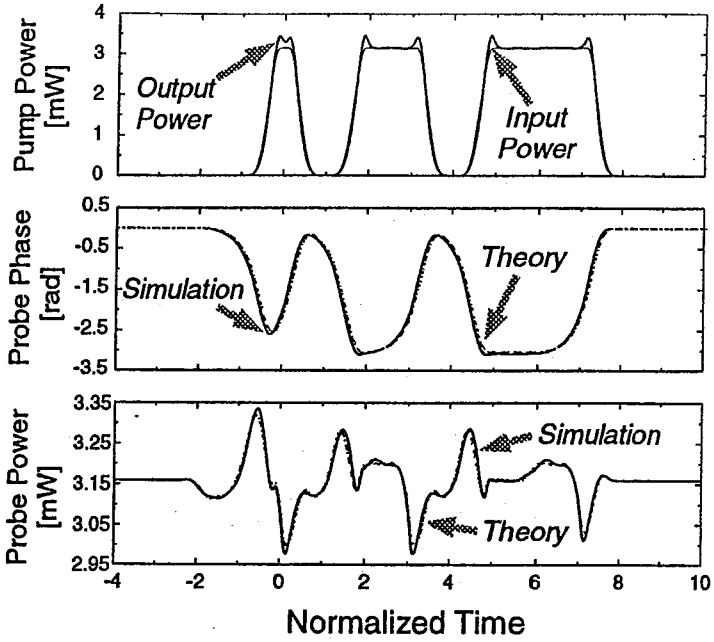

Fig. 5. Simulations of a NZDF compensated system, $R = 10$ Gb/s, $M = 10$ spans, $\Delta\lambda = 0.8$ nm. Top row: Pump power [mW]. Center row: Phase of probe signal [radians]. Bottom row: Power of probe signal. Time is normalized to the bit time 1/R.

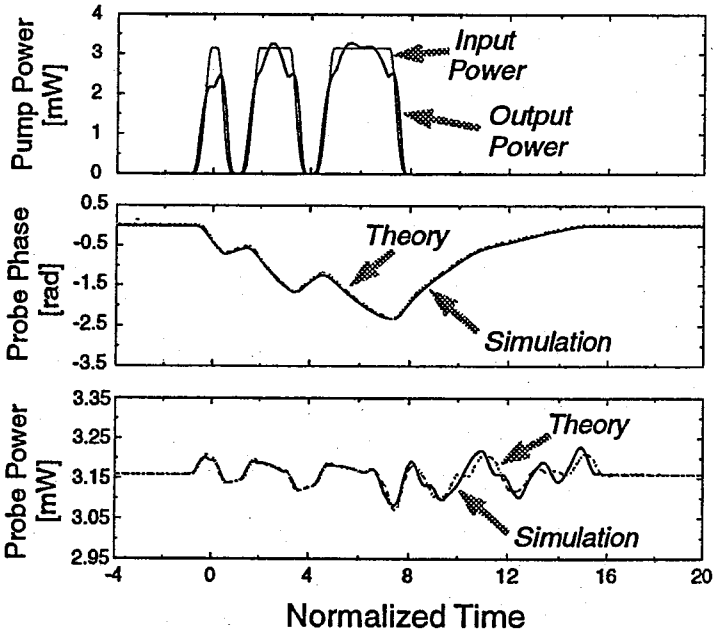

Fig. 6. Simulations of a SMF compensated system, $R = 10$ Gb/s, $M = 10$ spans, $\Delta\lambda = 0.8$ nm. Top row: Pump power [mW]. Center row: Phase of probe signal [radians]. Bottom row: Power of probe signal. Time is normalized to the bit time 1/R.

57 km, and a dispersion compensating fiber (DCF) with $D = -95$ ps/nm/km and length $l = 10.2$ km is used for compensation.

In both figures, the wavelength of exact compensation is halfway between channels.

Other parameters common to the two figures are: channel spacing $\Delta\lambda = 0.8$ nm, dispersion slope for all fibers $D' = 0.07$ ps/km/nm^2, nonlinear coefficient $\gamma = 2.35$ W^{-1} km^{-1}, attenuation $\alpha = 0.21$ dB/km.

The figures show the power of the pump both at the input and at the output of the link (top), the output phase of the probe both simulated and predicted by (14) (center), and the output power of the probe, both simulated and predicted by (18) (bottom) at the end of the system. The pattern "10110111" is visible in the pump intensity.

Such figures first show how accurate the predictions on the phase (IM/XPM model) are even when the underlying assumption of undistorted field envelopes used to derive the model is strongly violated. In fact, in both simulations the pump intensity distortion induced by GVD is quite evident, whereas in the probe phase the match between theory and simulations was so good that we had to displace the theoretical curves a little to make them visible. The good match is due to the lowpass filtering effect connected to GVD-induced channel walk-off.

The bottom figures also show the accuracy of the prediction on the probe intensity (IM/XPM/IM model).

Recall that the IM/XPM/IM model has been derived under two major hypotheses: the one previously discussed of undistorted field envelope, and the one of small perturbations upon which the model in [3] is based.

Though both hypotheses are violated, again we can see a good match between simulation and theory. This fact confirms that our model, however approximated, captures quite well the essence of the joint effect of XPM and GVD in compensated systems.

V. Conclusions

In future high-speed IM/DD WDM transmission systems with appropriate dispersion management, after FWM has been properly suppressed, the main cause of eye closure and thus of system degradation will be the two remaining nonlinear Kerr effects, SPM and XPM.

It is thus important to be able to accurately predict XPM, in order to estimate its local perturbation of the dispersion compensation, which gives rise to the residual intensity distorsion and thus eye closure.

This paper has given a time-domain derivation of the very important model for IM/XPM presented in [1]. A simple and very general expression for the impulse response of the XPM filters in the model has been presented.

While such filters are obtained in the assumption of undistorted field intensities on all channels, simulation results show that the model still accurately predicts the XPM even in the presence of strong intensity distortion.

This unobvious result implies that the modulation induced on the optical field phase by XPM is nearly independent of the distortion induced on the intensity of the optical field by group velocity dispersion.

The explicit expression of the IM/XPM filter impulse response is essential for instance to analytically evaluate the spectral broadening due to XPM in multi-span compensated systems [11].

The clear understanding of the decoupling between XPM and GVD-induced intensity distortion has formed the basis of our new IM/XPM/IM model to predict the signal intensity at the end of the compensated system. The model captures the essence of interaction between XPM and GVD, giving quite accurate predictions.

Acknowledgments

This work was supported partly by the European Community under INCO-DC project No. 950959 "DAWRON", and partly by a grant from CSELT.

References

[1] T. Chiang, N. Kagi, M. E. Marhic, and L. Kazovsky, "Cross-phase modulation in fiber links with multiple optical amplifiers and dispersion compensators," *IEEE J. Lightwave Technol.*, vol. 14, pp. 249-260, Mar. 1996.

[2] D. Marcuse, A. R. Chraplyvy, and R. W. Tkach, "Dependence of cross-phase modulation on channel number in fiber WDM systems," *IEEE J. Lightwave Technol.*, vol. 12, pp. 885-890, May 1994.

[3] J. Wang, and K. Petermann, "Small signal analysis for dispersive optical fiber communication systems," *IEEE J. Lightwave Technol.*, vol. 10, pp. 96–100, Jan. 1992.

[4] D. Marcuse, *Theory of Dielectric Optical Waveguides*, Academic, 2nd Ed., 1991, Chapter 9.

[5] G. P. Agrawal, *Nonlinear Fiber Optics*, Academic, 2nd Ed., 1995, Chapter 7.

[6] C. Kurtzke, "Suppression of fiber nonlinearities by appropriate dispersion management," *IEEE Photon. Technol. Lett.*, vol. 5, pp. 1250–1253, Oct. 1993.

[7] A. R. Chraplyvy, A. H. Gnauck, R. W. Tkach, R. M. Derosier, C. R. Giles, B. M. Nyman, G. A. Ferguson, J. W. Sulhoff, and J. L. Zyskind, "One-third terabit/s transmission through 150 km of dispersion-managed fiber," *IEEE Photon. Technol. Lett*, vol. 7, pp. 89-100, Jan. 1995.

[8] C. Crognale, "Small signal frequency response of a linear dispersive single-mode fiber near zero first-order dispersion wavelength", *IEEE J. Lightwave Techol.*, vol. 15, pp. 482-489, Mar. 1997

[9] M. Varani, "Analisi degli effetti di self e cross-phase modulation in sistemi multicanale con compensazione di dispersione." Laurea Thesis, Università di Parma, in preparation.

[10] A. B. Carlson, "Communication Systems." Mc-Graw-Hill, 3rd ed., 1986, p. 406.

[11] G. Bellotti, C. Francia, and A. Bononi, "Spectral broadening due to cross-phase modulation (XPM) in OOK WDM transmission systems," in *Proc. LEOS'97 10th Annual Meeting*, San Francisco, CA, pp. 226-227, paper WAA3, 1997.